Desalination and Water Treatment
www.deswater.com
doi: 10.1080/19443994.2015.1055810

57 (2016) 13144–13156
June

Taylor & Francis
Taylor & Francis Group

Enhancement of waste activated sludge reduction potential by amalgamated solar photo-Fenton treatment

S. Kavitha[a,1], P. Karthika[a,1], J. Rajesh Banu[a], Ick Tae Yeom[b], S. Adish Kumar[a,*]

[a]*Department of Civil Engineering, Regional Centre of Anna University, Tirunelveli, Tamil Nadu, India, emails: cutekavibio@gmail.com (S. Kavitha), karthikaannauniv@gmail.com (P. Karthika), Tel. +91 9444215544; email: rajeshces@gmail.com (J. Rajesh Banu), Tel. +91 9841339016; email: adishk2002@yahoo.co.in (S. Adish Kumar)*
[b]*Department of Civil and Environmental Engineering, Sungkyunkwan University, Seoul, South Korea, email: yeom@skku.edu*

Received 21 October 2014; Accepted 22 May 2015

ABSTRACT

The solar photo-Fenton process, which is one of the advanced oxidation processes, offers a promising technology for minimization of excess sludge. This study assessed the effect of solar photo-Fenton treatment of waste activated sludge (WAS). The operating parameters, viz. pH, ferrous iron concentration and hydrogen per oxide were optimized as 3, 40 mg/L and 4 g/L. SCOD and TCOD were 380 mg/L and 1,700 mg/L at 4-h contact time. The effects of the three critical factors, viz. pH, ferrous iron concentration and hydrogen peroxide for pretreatment of WAS were simulated and evaluated using response surface methodology. This methodology has shown to be a valuable tool to model complex process such as the light-enhanced photo-Fenton reaction and to achieve optimum experimental parameters at minimal cost. Solar photo-Fenton process achieved 4.62% COD solubilization at 4-h contact time.

Keywords: Waste activated sludge; Solar photo-Fenton process; Soluble chemical oxygen demand; Mixed liquor suspended solids; Response surface methodology; Advanced oxidation process

1. Introduction

Sludge produced from biological wastewater treatment processes has noticeably increased in current decades owing to the quantitative and qualitative extension of wastewater treatment [1]. Excess sludge contains a lot of materials such as pathogens, parasite eggs and unstable organics. The discharge of untreated excess sludge would bring a heavy environmental burden. Therefore, it is critical to develop an effectual disposal technique to reduce excess sludge [2]. Even though a lot of treatment methods are available with their own advantages and disadvantages such as hydrodynamic disintegration [3] using acids or alkali [4]. Biological [5–7] advanced oxidation process (AOP) is the most promising and effective technology. Among the various methods on

*Corresponding author.

[1]These two authors have contributed equally in this work.

the basis of lysis cryptic growth of sludge, advanced oxidation for reducing sludge production has been successfully applied in practice.

AOP is a chemical oxidation process with hydroxyl radicals, which are very reactive, and short-lived oxidants. Hydroxyl radicals may be produced in systems using: ultraviolet (UV) radiation/hydrogen peroxide (H_2O_2), ozone/hydrogen peroxide, UV radiation/ozone, Fenton's reagent (ferrous iron-Fe^{2+} and hydrogen peroxide), titanium dioxide/UV radiation and through other means. Production of UV radiation by lamps is expensive. Therefore, investigation is focusing increasingly on the AOPs, which can be powered by solar radiation, i.e. light with a wavelength greater than 300 nm, which are homogeneous catalysis by the photo-Fenton reaction. Therefore, the present work focusses on photo-Fenton process.

The photo-Fenton reaction is one of the AOPs which has been used to improve the dewatering of sludge. The application of the photo-Fenton reaction to minimize the excess activated sludge is based on the idea that part of activated sludge is mineralized to carbon dioxide and water while part of sludge is solubilized to organics. When applying Fenton processes for sludge disintegration, mineralization and solubilization occur [8]. Solar photo-Fenton process has been studied in order to increase the rate of the process and also improve degradation of solid wastes.

It can be expected that the photo-Fenton reaction destructs bacterial cell membranes, discharges biomass particulates and transform them into soluble components such as proteins, lipids and polysaccharides [9]. The foremost objectives of this study are (1) to disrupt the microbial biomass with solar photo-Fenton process, (2) to increase the sludge reduction and solubilization, (3) to study the kinetics of sludge treatment system, (4) to design solar photo-Fenton pilot scale processes for sludge treatment system and (5) to estimate cost analysis for solar photo-Fenton processes for the treatment of sludge.

2. Materials and methods

2.1. Collection of sample

The waste activated sludge (WAS) was collected from secondary clarifier of a municipal wastewater treatment plant in Trivandrum, Kerala. The sludge was concentrated by settling and stored at 4°C for 24 h. From the diluted sludge, the initial characteristics have been characterized before and after treatment and summarized in Table 1.

2.2. Effect of operating parameters for solar photo-Fenton treatment process

The effects of operating parameters such as pH, Fe^{2+}, H_2O_2 and contact time on COD solubilization and MLSS reduction were determined, and the various operating parameters were analysed and optimized.

2.2.1. Effect of pH

Five hundred milli litres of WAS was taken in four 2-L solar photo-Fenton reactors. The experiments were conducted by varying the pH in the range of 2–5 and the reaction was carried out for 0–4 h with the dosage of Fe^{2+} 40 mg/L and H_2O_2 4 g/L. The sample was taken at every 1 h and analysed for COD solubilization and MLSS reduction. After fixing the optimized pH, other parameters were changed and studied.

2.2.2. Effect of H_2O_2

Five hundred milli litres of WAS was taken in four 2-L solar photo-Fenton reactors. The experiments were conducted by varying the dosage of H_2O_2 in the range of 2–5 g/L and the reaction was carried out for 0–4 h with the constant dosage of Fe^{2+}. The sample was taken at every 1 h and analysed for COD solubilization and MLSS reduction.

Table 1
Characterization of sludge before and after treatment

S. no.	Sludge characteristics	Before treatment	After treatment
1	TCOD	8,000 ± 510 mg/L	1,600 ± 120 mg/L
2	SCOD	100 ± 5.45 mg/L	395 ± 15 mg/L
3	MLSS	4,500 ± 210 mg/L	895 ± 25 mg/L
4	VSS	3,800 ± 210 mg/L	230 ± 15 mg/L
5	TDS	2,580 ± 120 mg/L	2,670 ± 130 mg/L
6	pH	3 ± 0.5	2.6 ± 0.5

2.2.3. Effect of Fe^{2+}

Five hundred milli litres of WAS was taken in four 2-L solar photo-Fenton reactors. The experiments were conducted by varying the dosage of Fe^{2+} in the range of 20–50 mg/L and the reaction was carried out for 0–4 h with the constant dosage of H_2O_2. The sample was taken at every 1 h and analysed for COD solubilization and MLSS reduction.

2.2.4. Effect of contact time

Five hundred milli litres of WAS was taken in four 2-L solar photo-Fenton reactors. The experiments were conducted by varying the contact time 0–4 h with the constant dosage of H_2O_2 and Fe^{2+}. The sample was taken at every 1 h and analysed for COD solubilization and MLSS reduction.

2.3. Experimental design of solar photo-Fenton for treatment of WAS by response surface methodology

The study of a process often focuses on the relationship between the system response and the input factors. Typical motivations for such a study are the need for optimization of a process or the intent of understanding the underlying mechanisms in the system. To describe the relation between a system response and input factors typically, a mathematical model is formulated. The combination of experimental design and formulation of a mathematical model to yield a quantitative description of the response over a whole experimental region in a system with n continuous input factors is called response surface methodology (RSM), because the system response can be described by a continuous surface in the n dimensional factor space [10]. Usually, the input factors are scaled in such a way that the minimum value of the respective factor of the investigated region is −1 and the maximum value is +1. A class of three levels of complete Box–Behnken design for the estimation of parameters in a second-order mode was developed by Box–Behnken. Basically, the optimization process involves three major steps, which include performing the statistically designed experiments, estimating the coefficients in a mathematical model and predicting the response and checking the adequacy of the model. The effect of several factors influencing the COD solubilization, such as pH value of the sludge and Fe^{2+} concentration were chosen as the critical variables and designated as A, B and C, respectively. The three significant independent variables A, B, C and the mathematical relationship of the response Y on these variables can be approximated by a second-degree polynomial equation (Eq. (1)) [11].

$$Y = \beta 0 + \beta 1A + \beta 2B + \beta 3C + \beta 12AB + \beta 13AC + \beta 23BC + \beta 11A^2 + \beta 22B^2 + \beta 33C^2 \quad (1)$$

The regression equation obtained after analysis of variance (ANOVA) gives the level of COD solubilization as a function of different concentration of Fe^{2+}, pH and H_2O_2. Regression mode containing three linear (A, B and C), three quadratic (A^2, B^2 and C^2) and three interaction terms plus one block term was employed using the design expert. The design was performed because relatively few experimental combinations of the variables were needed to estimate potentially complex response functions. A total of 17 experiments were necessary to estimate the 10 coefficients of the model using multiple linear regression analysis. Eq. (1) was solved using the design expert (Stat-Ease Inc. version 7) to estimate the response of the independent variables. The maximum predictable response for COD solubilization was also obtained.

2.4. Treatability studies

Treatability studies on solar photo-Fenton was studied in a 2-L reactor of length 25 cm, width 15 cm and depth 5 cm containing 500 mL of WAS under optimum conditions at pH 3, Fe^{2+} dosage of 40 mg/L, H_2O_2 dosage of 4 g/L and time 4 h for high solubilization of COD and reduction of MLSS.

The extent of MLSS reduction during the experiment was calculated by the equation mentioned below:

$$\text{MLSS reduction } (\%) = [(\text{Initial} - \text{Final})/\text{Initial}] \times 100 \quad (2)$$

The efficiency of the sludge pretreatment was measured in terms of the COD solubilization effectiveness and was calculated by the following (Eq. (3)):

$$\alpha = \frac{(\text{SCOD}_\text{p} - \text{SCOD}_\text{i})}{(\text{TCOD}_\text{i} - \text{SCOD}_\text{i})} \quad (3)$$

where α = solubilization efficiency (%), SCOD_p = SCOD concentration of the sludge after disintegration (mg/L), SCOD_i = SCOD concentration of the sludge before disintegration (mg/L), and TCOD_i = TCOD concentration of the sludge before disintegration (mg/L).

2.5. Design of pilot-plant system and treatment cost estimation

The design of solar photo-Fenton system was done for treating 1.25×10^{-3} m^3/min containing inlet sludge concentration of 4,500 mg/L. Design was done based on the reactor configuration, rate constant, i.e. kinetics of the process, desired destruction level or destruction and removal efficiency. Total cost of the treatment plant was calculated by including capital cost and operating cost. The capital cost includes cost of reactor, storage and settling tanks, piping, fittings, pumps, blowers, controls, installation, auxiliary and capital contingency. The operational and maintenance cost includes catalyst, oxidant and maintenance.

2.6. Analytical parameters

Analytical parameters such as MLSS, SCOD and TCOD were measured according to the standard methods [12]. pH was measured using a digital pH metre.

3. Results and discussion

3.1. Effect of operating parameters for solar photo-Fenton treatment process

The effectiveness of operational parameters such as pH, H_2O_2 dosage, ferrous sulphate dosage and contact time for solar photo-Fenton reaction was appraised based on SCOD release and MLSS reduction. In fact, under acidic conditions, Fe^{2+}/H_2O_2 mixture produces OH radicals. The Fenton reaction produces the hydroxyl radical in acidic solutions by iron catalysed decomposition of H_2O_2. These radicals have an oxidizing potential and are capable of oxidizing a wide range of organics [13–15].

3.1.1. Effect of pH on SCOD release and MLSS reduction for solar photo-Fenton process

The sludge pH is one of the most imperative functioning parameters, which is directly affecting the oxidation capability of the Fenton process. The effect of pH on SCOD release and MLSS reduction during solar photo-Fenton reaction is depicted in Fig. 1(a) and (b). The experiments were performed in the pH of 2, 3, 4 and 5 by maintaining other process parameters constant.

The pH of the solution controls the production rate of OH radical and the concentration of Fe^{2+}. From the Fig. 1(a), it was observed that the SCOD release was more up to pH 3. At pH 3, the SCOD release was found to be 370 mg/L. After that, there was a decline

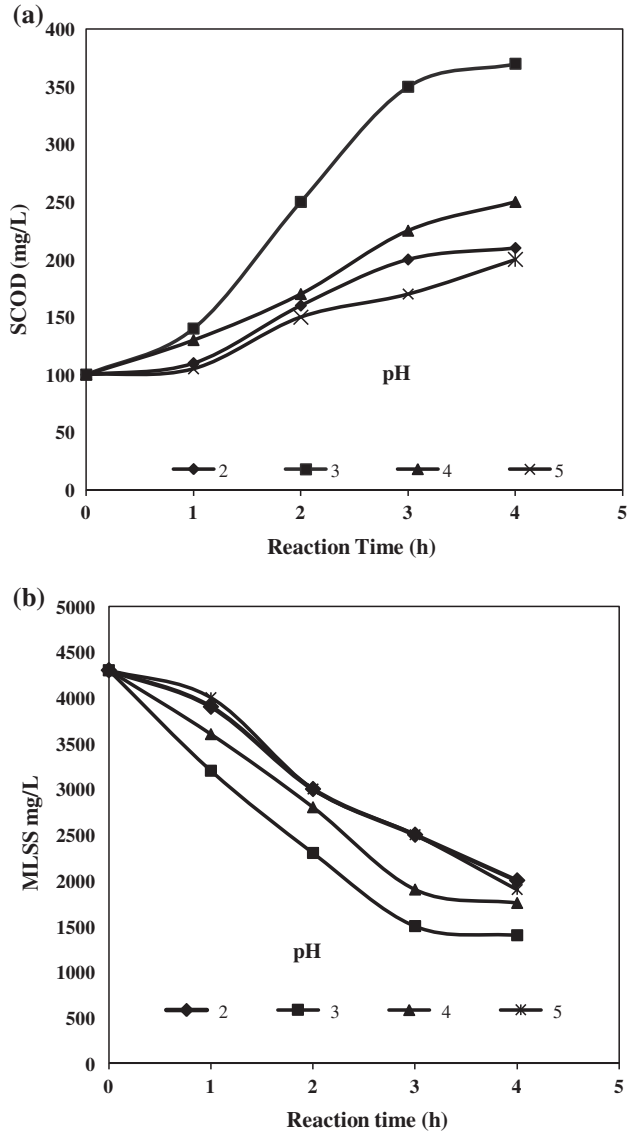

Fig. 1. Optimization of pH based on SCOD and MLSS. (a) Effect of pH on SCOD release and (b) effect of pH on MLSS reduction.

in SCOD release. Photo-Fenton reactions make use of the reactivity of the hydroxyl radical produced in acidic solution. This decrement was due to two main bases: for pH 4 and 5, iron precipitates as $Fe(OH)_3$ and dissolved iron concentration is fairly low. As a result, its potential ability to catalyse H_2O_2 was lowered. This indicates that organic compounds might be destructed in homogeneous aqueous phase above the pH 3. This outcome is consistent with the results of Sahinkaya et al. [16].

The pH has a significant role in determining the competency of Fenton and photo-Fenton oxidation. Therefore, the specified initial pH of the WAS was

adjusted to 3 which is the optimal value for the photo-Fenton reaction using sulphuric acid [17]. Similar to SCOD release, the MLSS reduction was more in pH 3. At initial, the MLSS was found to be 4,300 mg/L.

After adjusting the pH of the sludge to 3, the MLSS was reduced to 1,400 mg/L, respectively, which is clearly represented in Fig. 1(b). After that, there was no significant increase in MLSS reduction. Acidification caused iron hydroxides, phosphates and other water retentive salts to dissolve. As a result, a large part of the organic matter is also dissolved during the acidification. Therefore, based on SCOD release and MLSS reduction, the optimum pH for photo-Fenton reaction was found to be 3.

3.1.2. Effect of H_2O_2 dosage on SCOD release and MLSS reduction for solar photo-Fenton process

Fig. 2(a) and (b) depicts the effects of H_2O_2 concentration on sludge solubilization and reduction at different H_2O_2 concentrations (2–4 g/L). The increase in H_2O_2 concentration up to 4 g/L was found to enhance the sludge disintegration rate. At 4 g/L dosage of H_2O_2, the SCOD release was found to be 300 mg/L. The initial MLSS was found to be 4,300 mg/L. At 4 g/L dosage of H_2O_2, the MLSS concentration reduced to 1,400 mg/L. Further increasing the H_2O_2 dosage, no significant increase in SCOD release and MLSS reduction was observed. At high H_2O_2 concentration, there is a competition between the organic substances and H_2O_2. At high concentrations, hydrogen peroxide itself may act as a free-radical scavenger in secondary reactions, causing a decrease in the hydroxyl radical concentration [18]. This might be the reason for decreased SCOD release and MLSS at H_2O_2 dosage 5 g/L. Hydrogen peroxide was consumed at a fast rate initially, and subsequently, the rate of H_2O_2 consumption was somewhat decreased.

3.1.3. Effect of Fe^{2+} dosage on SCOD release and MLSS reduction for solar photo-Fenton process

The effect of Fe^{2+} dosage on the solubilization and degradation of sludge is illustrated in Fig. 3(a) and (b). The MLSS reduction and SCOD release was increased with increasing Fe^{2+} dosage up to 40 mg/L. At 40 mg/L dosage of ferrous sulphate, the SCOD release and MLSS concentration were found to be 378 mg/L and 1,440 mg/L, respectively. Beyond that dosage, no noteworthy differences have been observed in SCOD release and MLSS reduction. Therefore, 40 mg/L of ferrous sulphate was considered to be optimum dosage for the subsequent process.

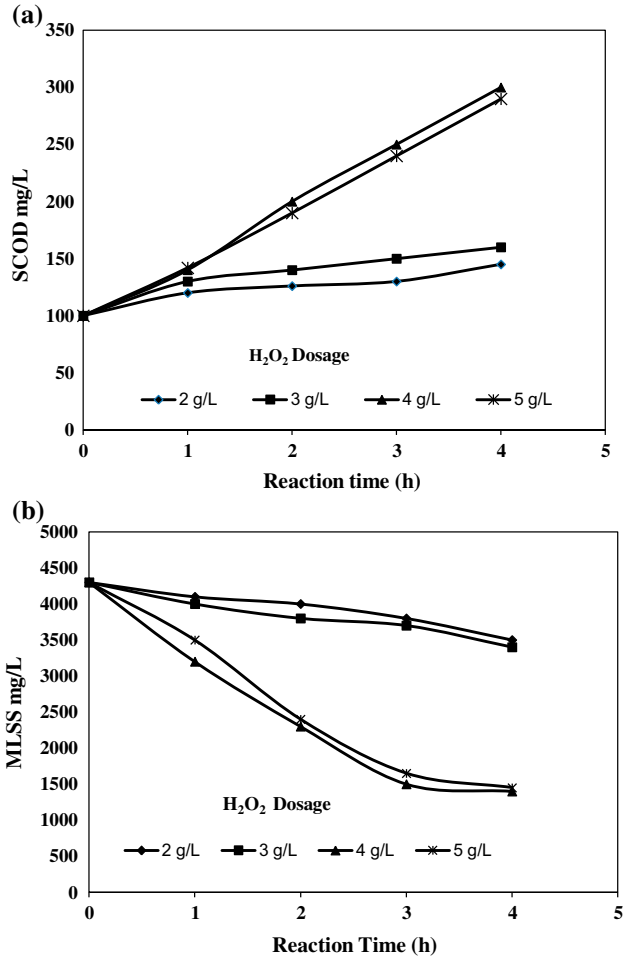

Fig. 2. Optimization of H_2O_2 dosage based on SCOD and MLSS. (a) Effect of H_2O_2 dosage on SCOD release and (b) effect of H_2O_2 dosage on MLSS reduction.

The increase in MLSS reduction and SCOD release up to 40 mg/L dosage of Fe^{2+} is due to the generation of hydroxyl radicals. Similarly, the SCOD release was more up to 40 mg/L dosage of ferrous sulphate.

3.1.4. Effect of contact time on SCOD release and MLSS reduction for solar photo-Fenton process

Similar to pH, H_2O_2 dosage, Fe^{2+} dosage, contact time also plays a major role in Fenton process. Fig. 4 depicts the variation of SCOD and MLSS with respect to contact time in photo-Fenton reaction with the initial sludge concentration of 4,300 mg/L, the Fe^{2+} concentration of 40 mg/L, the initial H_2O_2 concentration of 4 g/L, initial solution pH of 3 and in the presence of solar light. From the figure, it was observed that that the chemical oxidation by photo-Fenton reaction could be roughly divided into two phases (Phases

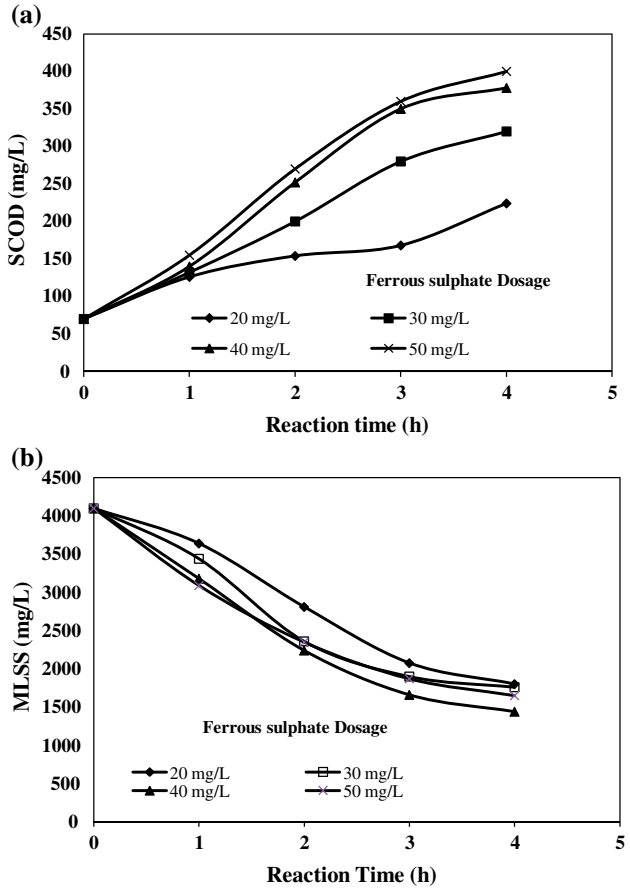

Fig. 3. Optimization of ferrous sulphate dosage based on SCOD and MLSS. (a) Effect of ferrous sulphate dosage on SCOD release and (b) effect of ferrous sulphate dosage on MLSS reduction.

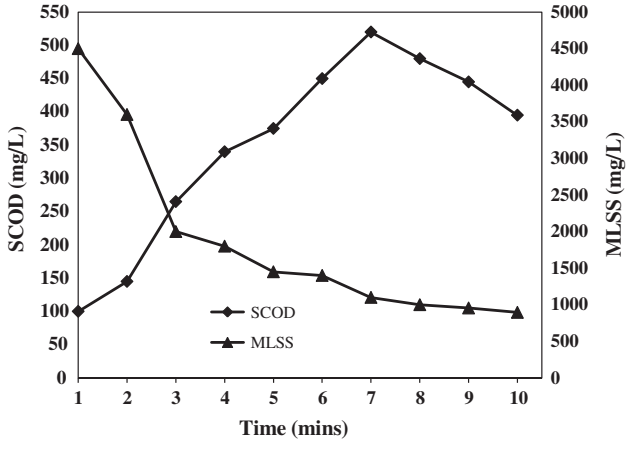

Fig. 4. Optimization of contact time based on MLSS and SCOD.

1 and 2). From Fig. 4, it was observed that in Phase 1, the concentration of SCOD increases with increment in contact time up to 7 h. At 7 h, the concentration of SCOD was found to be 530 mg/L.

As a result of this combined treatment, organic substances were leached into the supernatant and as a result there is increment in soluble COD [19,20] up to 7 h. After that, the concentration of soluble COD was decreased (Phase 2). In Phase 1, the soluble COD was increased. On the other hand, in Phase 2, there is a net competition between initial release rate and final mineralization rate. As a result, the initial release rate was exceeded by the final mineralization rate which might be the reason for decrement of soluble COD after 7 h. This change in dissolved COD is similar to the results of Egemen et al. [20]; Vlyssides [21]; Déléris et al. [22].

Analogous to SCOD release, the concentration of MLSS was also reduced up to 7 h. From the figure, it was noted that the MLSS was found to be decreased from 4,500 to 895 mg/L after 9 h of photo-Fenton reaction with the initial H_2O_2 concentration of 4 g/L. Up to 7 h, the decrement in MLSS was rapid. After 7 h, only negligible concentration of MLSS was reduced. The rapid reduction of MLSS was ceased within 7 h. First, the decrease in MLSS occurred rather significantly and then sluggishly. Ferrous ion catalyses H_2O_2 to form OH radical quickly in the first stage of reaction itself (up to 7 h). This might be the reason for rapid release of SCOD and reduction of MLSS up to 7 h.

3.2. Optimization of solar photo-Fenton process for the treatment of WAS by RSM

RSM is a sequential procedure with an initial objective to lead the experiments rapidly and efficiently along a path of improvement towards the general vicinity of the optimum. The parameters investigated were pH, H_2O_2 dosage and Fe^{2+} dosage. All parameters were taken at a central coded value considered as zero and studied at three different levels (−1, 0, +1). In this case, a three level Box–Behnken design resulting in a total number of 17 experiments was employed to fit the second-order polynomial model. The statistical combinations of the critical parameters along with the maximum observed and predicted COD solubilization efficiency are listed in Table 2.

The predicated COD solubilization values are very close to the observed ones in all set of experiments. The highest efficiency of 4.62% and the lowest efficiency of 2.7% were observed. Table 3 shows the results of the quadratic response surface model fitting in the form of ANOVA.

ANOVA is required to test the significance and adequacy of the model. The mean squares are obtained by dividing the sum of squares of each of

Table 2
Box–Behnken design matrix for three test variables in coded and natural units along with the observed responses

Experiment no.	*A*	*B*	*C*	pH	Amount of Fe (mg/L)	H_2O_2 (g/L)	COD solubilization (%) Observed	COD solubilization (%) Predicted
1	−1	−1	0	3	40	4	4.62	3.79
2	+1	−1	0	3	40	4	4.62	4.62
3	−1	+1	0	3	45	4.5	4.25	3.82
4	+1	+1	0	3	45	3.5	4.01	3.33
5	−1	0	−1	2	35	4	3.50	3.81
6	+1	0	−1	3	35	3.5	3.70	2.87
7	−1	0	+1	4	40	4.5	3.14	3.19
8	+1	0	+1	4	45	4	3.3	3.40
9	0	−1	−1	2	40	4.5	3.5	4.13
10	0	+1	−1	3	35	4.5	3.6	3.23
11	0	−1	+1	2	40	3.5	3.5	3.32
12	0	+1	+1	4	35	4	3	3.47
13	0	0	0	3	40	4	4.62	2.71
14	0	0	0	3	40	4	4.62	4.05
15	0	0	0	3	40	4	4.62	3.72
16	0	0	0	4	40	3.5	2.7	3.96
17	0	0	0	2	45	4	2.9	4.24

Table 3
ANOVA for solar photo-Fenton treatment process using RSM

Source of variations	Sum of squares	Degree of freedom	Mean square	*F*-value	Probability *p* (>*F*)
Model	6.91	9	0.77	15.36	0.0008
Residual	0.35	7	0.050		
Lack of fit	0.35	3	0.12		
Error	0.00	4	0.000		
Corrected total	7.26	16			

the two sources of variation, the model and the error variance, by the respective degrees of freedom. The Fisher variation ratio, the *F*-value ($= S_r^2/S_e^2$), which is a statistically valid measure of how well the factors describe the variation in the data about its mean can be calculated from ANOVA by dividing the mean square due to model variation by that due to error variance. The greater the *F*-value is from unity, the more certain it is that the factors explain adequately the variation in the data about its mean, and the estimated factor effects are real. The ANOVA of the quadratic regression model demonstrates that the model is highly significant, as is evident from the Fisher *F*-test ($F_{model} = 15.36$) and a very low probability value ($P_{model} > F = 0.0500$). The probability *p*-value is relatively low, indicating the significance of the model. Moreover, the computed *F*-value is much greater than the tabular *F*-value at 1% level, indicating that the treatment differences are highly significant. This fit of the model was further checked by the coefficient of determination R^2. The R^2-values provide a measure of how much variability in the observed response values can be explained by the experimental factors and their interactions. The R^2-value is always between 0 and 1. If the R^2 values lies in between 0.75 and 0.99, the fitted regression equation is considered good fit of the model. When expressed as percentage, R^2 is interpreted as the per cent variability in the response explained by the statistical model.

In this study, the value of the determination coefficient ($R^2 = 0.9518$), indicating that 95.18% of the variability in the response could be explained by the model. As well, the adjusted determination coefficient (adjusted $R^2 = 0.8898$) is also very high to advocate for a high significance of the model. These ensured a satisfactory adjustment of the polynomial model to the experimental data. The adjusted R^2 corrects the R^2-value for the sample size and the number of the terms in the model. If there are many terms in the model and the sample size is not large, the adjusted R^2 may be noticeably smaller than the R^2. Here, the adjusted R^2 was smaller than the R^2 value [23].

The application of RSM offers on the basis of parameter estimate, an empirical relationship between the COD solubilization efficiency and the test variables under consideration. The response variable and the test variables are related by the following quadratic expression (Eq. (4)).

$$Y = 4.62 + 0.082A + 0.072B - 0.16C + 0.085AB + 0.23AC + 0.11BC - 0.38A^2 - 0.38B^2 - 1.06C^2 \quad (4)$$

where Y is the response, which is the COD solubilization efficiency expressed in % and A, B and C are the coded values of Fe, H_2O_2 and pH, respectively. The p-values were used as a tool to check the significance of each of the coefficients, which in turn are necessary to understand the pattern of the mutual interaction between the test variables. The larger the magnitude of the t-value and smaller the p-value, the more significant is the corresponding coefficient. The parameter estimate and the corresponding p-values suggest that among the test variables, initial pH produces the largest effect on COD solubilization efficiency.

Response surface plots provide a method to predict the COD solubilization efficiency for different values of the tested variables and the contours of the plots help in identification of the type of interactions between these variables. Each contour curve represents an infinite number of combinations of two tested variables with the other two maintained at their respective zero level.

A circular contour of response surface indicates that the interaction between the corresponding variables is negligible. In contrast, an elliptical or saddle nature of the contour plots indicates that the interaction between the corresponding variables is significant. The response surface contour plots for the effect of each pair of variables are shown in Figs. 5a, 5b and 5c. Each contour curve represents an infinite number if combinations of two test variables with the other two maintained at their respective zero level.

The normal probability plot of the studentized residuals indicates that none of the individual residual exceeded the residual variance (twice the square root of the residual variance) and that an excellent adequacy of the regression model was utilized. It further proves that the experimental values are in good agreement with the predicted values. Table 4 shows the maximal efficiency of COD solubilization, by the critical value of each parameter, which was predicted from the data analysis with the statistical technique.

After verifying by further experiment test with the predicated values, the results indicated that the maximum COD solubilization efficiency was obtained when the values of each parameter were set as the critical values, which is in good agreement with the value predicted from the regression model.

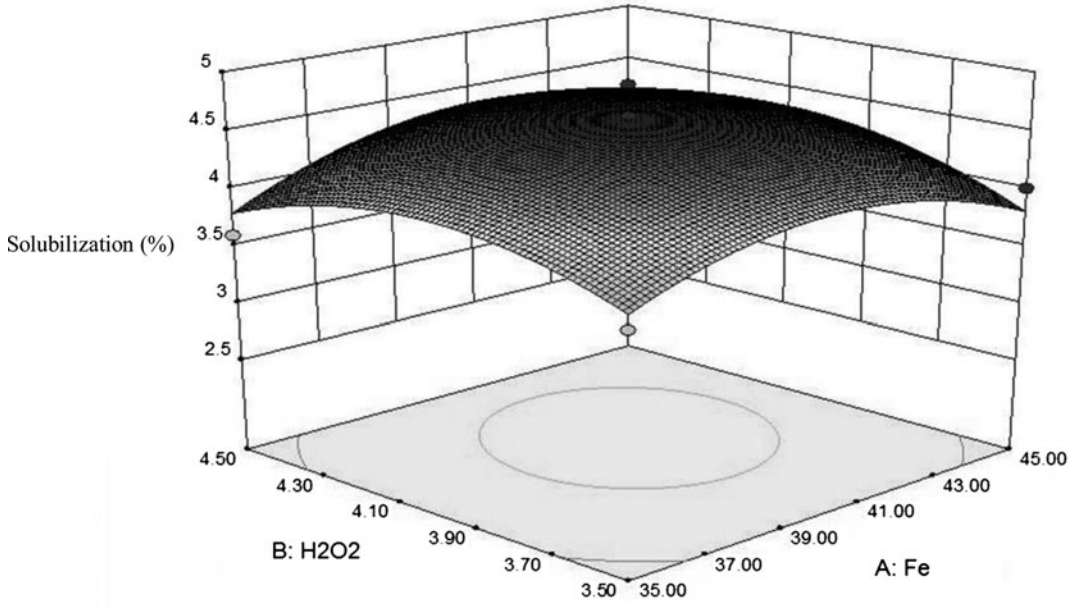

Fig. 5a. Response surface optimization of COD solubilization vs. Fe and H_2O_2.

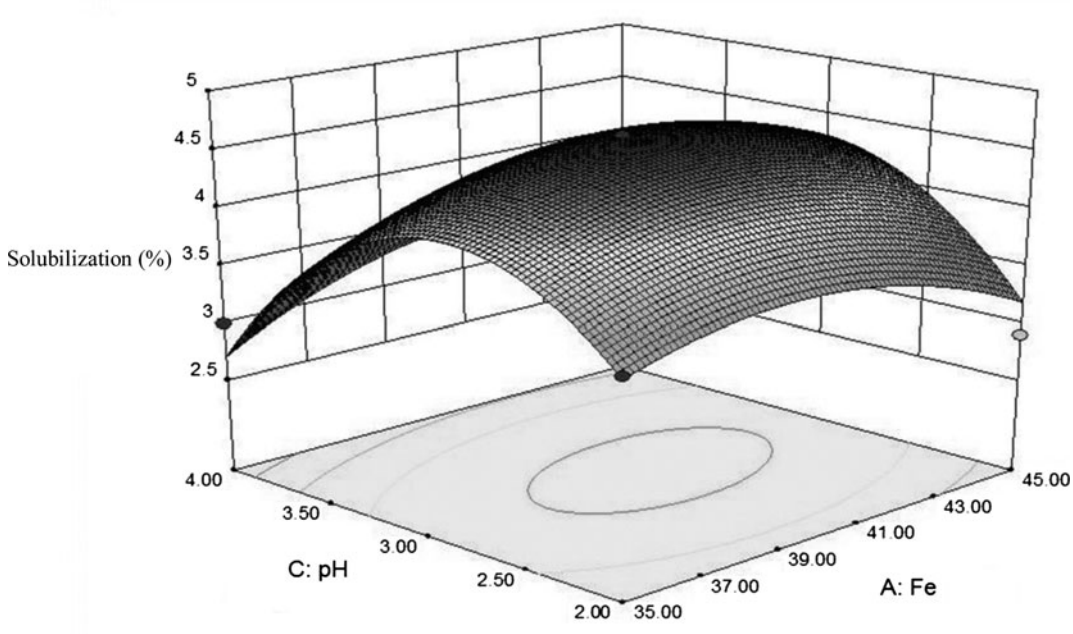

Fig. 5b. Response surface optimization of COD solubilization vs. Fe and pH.

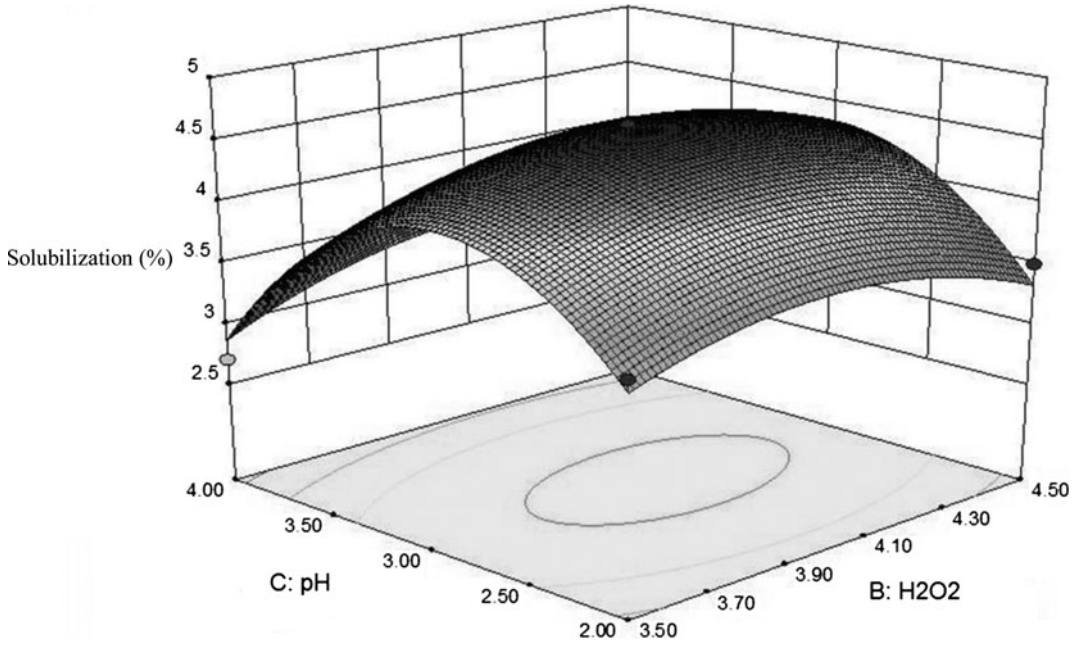

Fig. 5c. Response surface optimization of COD solubilization vs. H_2O_2 and pH.

3.3. Effect of solar photo-Fenton process

In order to compare the efficiency of various processes and to study the effect of solar irradiation and Fenton process, five sets of experiments were conducted, viz. only H_2O_2 (without Fe^{2+}), only Fe^{2+} (without H_2O_2), only UV irradiation (solar) and (solar photo-Fenton). The results of the experimental studies were depicted in Fig. 6. In the presence of solar light without Fenton's reagent (Fe^{2+} and H_2O_2 dosage), only slight increment in COD solubilization (1.5%) was

Table 4
The critical values of variables for the optimal COD solubilization

Parameters	Critical values
pH	3
H_2O_2 (g/L)	4
Fe^{2+} (mg/L)	40
Predicated solubilization efficiency	4.65
Observed solubilization efficiency	4.62

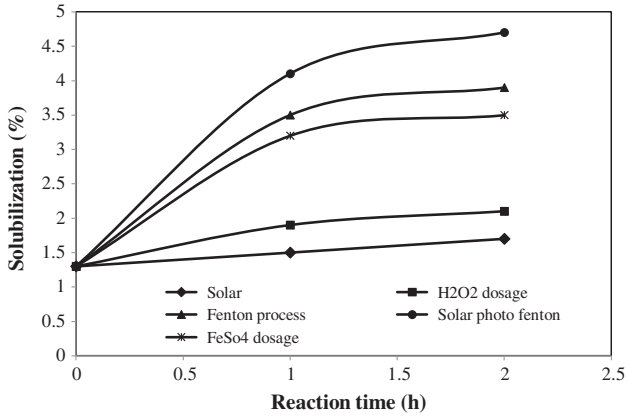

Fig. 6. Effects of UV light irradiation and Fenton reagents on sludge solubilization (initial MLSS = 4,500 mg/L, Fe^{2+} dosage 40 mg/L and H_2O_2 dosage 4 g/L).

obtained. The COD solubilization was found to be 3.5% with Fe^{2+} dosage alone. In solar photo-Fenton process, COD solubilization was found to be 4.7%. With H_2O_2 dosage, the COD solubilization was found to be 2.1%, whereas in Fenton process, the COD solubilization was found to be 3.9%. By the addition of H_2O_2, only slight increment in COD solubilization was observed. Since the H_2O_2 concentration was directly related to the number of OH radicals generated in the photo-assisted Fenton reaction, the OH radicals were not generated without H_2O_2. It is because the hydroxyl radicals could not be produced in the Fe^{2+}/solar system alone, and then, the direct photolysis of the sludge was very limited. Therefore, further increment in COD solubilization was due to OH radicals generated by H_2O_2 that plays a major role in COD solubilization.

It is clear from the results presented in Fig. 6 that simultaneous utilization of solar light irradiation with Fenton's reagent increased the decomposition of activated sludge. A substantial increase in the COD solubilization (4.7%) was observed in solar photo-Fenton reaction, and subsequently, the COD solubilization reached a maximum at 7-h treatment and beyond that point, the COD solubilization was decreased which is clearly depicted in Fig. 4.

3.4. Solar photo-Fenton treatment kinetics based on SCOD release

The treatment of sludge improved by solar photo-Fenton reaction has been investigated and the effect of treatment of sludge were reported to play an important role in the solubilization of biodegradable organic matter. In this study, the solar photo-Fenton reaction was used for the treatment and their role in cell disintegration was investigated and the kinetic parameters were evaluated.

During sludge treatment by solar photo-Fenton reaction in batch test, the changes in soluble COD with respect to time were observed. The cumulative effects of these changes were simplified to single first-order kinetics. The SCOD changes of solar photo-Fenton pretreated sludge were increased up to 6 h. Clearly, the slope of the curve indicated the changes of SCOD per unit time. Accordingly, the slope of points on the curve represented the reaction rate of corresponding time. Based on these results, the effect of solar photo-Fenton treatment on SCOD release within the 7 h could be expressed by first-order kinetics.

The rate constant for SCOD release of solar photo-Fenton pretreated sludge was found to be 70.714 h^{-1}. The R^2 value of treatment process was found to be 0.98 which indicates that there is an optimistic relationship between the model and experimental design. Hence, the model fitted the experimental facts adequately.

3.5. Design of pilot plant

A solar photo reactor operated in the batch, recirculating mode is analysed in terms of very simple observable variables such as the impinging photon flux, the incident area, the initial concentration (even if they have to be expressed as COD values), the flow rate, the reactor volume and incident radiation fluxes and a fairly simple experimental determination such as the observed photonic efficiency. The analysis is formulated in terms of the photon input corresponding to an equivalent batch system that is derived as a new reaction coordinate for photoreactions. Employing several plausible approximations, the pollutant concentration evolution in the tank is cast in terms of very simple analytical solutions.

In the treatment performance studies, a kinetic model which accounts the effect of sludge concentration, sludge volume, light intensity and area of solar irradiation was used to arrive at a lump kinetic parameter (K_3) (Eq. (5)) as suggested by Sagawe et al. [24].

$$K_3 = \ln(C_0/C) \times Q/(q_{UV} \times A) \quad (5)$$

where K_3 = lump kinetic parameter representing the efficiency of the photo-Fenton (m^3/W min), C_0 = inlet concentration of sludge (mg/L), C = outlet concentration of sludge (mg/L), Q = volumetric flow rate (m^3/min), q_{UV} = time averaged radiation density flux (W/m^2), A = effect area of solar irradiation (m^2), K_3 = ln (4,500/895) × 500/9 (mL/h)/(23 × 0.043), and $K_3 = 1.510 \times 10^{-6}$ (m^3/W min).

For, scaling up of the reactor.
$(K_3)_{\text{bench-scale reactor}} = (K_3)_{\text{pilot-scale reactor}}$.
Hence, $A_{\text{pilot-scale reactor}} = \ln (C_0/C) \times Q_{\text{pilot-scale reactor}}/(q_{UV}) \times (K_3)_{\text{bench-scale reactor}}$,

where K_3 = lump kinetic parameter (1.510×10^{-6} m^3/W min), C_0 = inlet concentration of sludge (4,500 mg/L), C = outlet concentration of sludge (895 mg/L), Q = volumetric flow rate of pilot plant (1.25×10^{-3} m^3/min), q_{UV} = time averaged radiation density flux (23 W/m^2).

$$A_{\text{pilot-scale reactor}}\ (m^2) = \ln(4,500/895) \times 1.25 \times 10^{-3}\ (m^3/\text{min}/23 \times 1.510 \times 10^{-6} = 58.12\ m^2$$

Therefore, the surface area (A) of the pilot plant reactor is 58.12 m^2.

3.6. Economic analysis

Cost is always a key topic when innovative technologies are considered, and standard commercial procedures indicate that any new technology should provide significant reductions in processing costs over competing technologies or significant new technical contributions for its successful marketing. The cost of sludge management is around 50% of the total operating cost of the wastewater treatment plant [25], and the profitable practicability of a treatment process is

Table 5
Cost estimation (USD) for treatment of WAS with solar photo-Fenton process

S. no.	Parameters	Values
1	*Common input data*	
	Yearly working days	365 d
	Availability factor	80%
	Average useful hours	9 h
	Effective yearly operating hours	2,628 h
	UV global radiation (average at operating hours)	23 W/m^2
	Total collector area	59
	Cost of solar photocatalytic reactor civil works	72/m^2
2	*Cost estimation*	
	(i) Direct cost	
	Total reactor cost (59 × 72)	4,248
	Piping and tanks (8% of reactor cost)	339
	Auxiliary equipment and controls (10% of reactor cost)	425
	Others (15% of reactor cost)	638
	Total direct cost (TDC)	5,650
	(ii) Indirect cost	
	Contingencies (12% of TDC)	678
	Spare parts (1% of TDC)	57
	Total capital required (TCR)	735
	(iii) Annual cost	
	Capital (13% of TCR)	96
	Consumables (FeSO4, H_2O_2)	2,115
	Operation and maintenance (5% of TCR)	37
	Total annual cost	2,248
	Treatment cost	6.23/m^3

thoroughly related to the enhancement in solubilization and solids reduction. In the case of solar photo-Fenton process, its main contribution is the environmental added value of using solar energy. The pretreatment techniques, namely thermal, chemical, mechanical and physical, and several combinations such as mechanical–chemical and thermal–chemical may be considered the main competitors of solar photo-Fenton treatment of WAS. Thermal pretreatment requires a considerable amount of heat to preheat the sludge, ultrasonication is no doubt the most powerful method to disrupt cell walls, but power consumption becomes a serious drawback, mechanical techniques do not require chemical or heat but consume a lot of power. Table 5 shows the estimated treatment cost of a solar photo-Fenton process. The overall cost of solar photo-Fenton oxidation for the treatment of 1 m^3 of WAS per day was estimated to be 6.23 USD/m^3. This cost is lower than for technologies such as microwave pretreatment (215 USD/m^3) [26], ultrasonic pretreatment (23.91 USD/m^3) [27], thermochemical pretreatment (87.6 USD/m^3) [28], thermochemical and disperser pretreatment (8.44 USD/m^3) [28] also with the important advantage that solar photo-Fenton process is a sludge treatment process, while the others are only pretreatment technologies. Based on the above-mentioned reports, it can be concluded that the solar photo-Fenton process was found to be economically viable from a cost-effective approach.

4. Summary and conclusion

Solar photo-Fenton process is relatively inexpensive method. The process can make use of sunlight instead of artificial light, which reduces the operating costs and it is eco-friendly to the environment. This study assessed the effect of solar photo-Fenton treatment of WAS. Results showed SCOD and TCOD were 380 mg/L and 1,700 mg/L at 4-h contact time. The effects of the three critical factors, viz. pH, ferrous iron concentration and hydrogen peroxide for treatment of WAS were simulated and evaluated using RSM. This methodology has shown to be a valuable tool to model complex process such as the light-enhanced photo-Fenton reaction and to achieve optimum experimental parameters at minimal cost.

Results showed the viability of the Fenton process in the treatment of sludge. In summary, evidence showed that solar photo-Fenton process achieved 4.62% COD solubilization. Results obtained from this research and the economic cost evaluation indicated that the solar photo-Fenton treatment could be an appropriate treatment method for enhancing degradability of sludge.

References

[1] Y.K. Kim, J.H. Bae, B.K. Oh, W.H. Lee, J.W. Choi, Enhancement of proteolytic enzyme activity excreted from *Bacillus stearothermophilus* for a thermophilic aerobic digestion process, Bioresour. Technol. 82 (2002) 157–164.

[2] T. Ying, Y. Yong, L. Xiao-ming, Y. Qi, W. Dong-bo, Z. Guang-ming, Isolation, identification of sludge-lysing thermophilic bacteria and its utilization in solubilization for excess sludge, Environ. Technol. 8 (2012) 961–966.

[3] R.R. Uma, S. Kaliappan, S. Adish Kumar, J. Rajesh Banu, Combined treatment of alkaline and disperser for improving solubilisation and anaerobic biodegradability of dairy waste activated sludge, Bioresour. Technol. 126 (2012) 107–116.

[4] R.J. Banu, D.K. Uan, S. Adish Kumar, I.T. Yeom, S. Kaliappan, A novel method of sludge pretreatment using the combination of alkalis, J. Environ. Biol. 33 (2012) 249–253.

[5] S. Gopi Kumar, J. Merrylin, S. Kaliappan, S. Adish Kumar, I.T. Yeom, J. Rajesh Banu, Effect of cation binding agents on sludge solubilization potential of bacteria, Bioprocess Eng. 17 (2012) 346–352.

[6] J. Merrylin, S. Adish Kumar, S. Kaliappan, I.T. Yeom, J. Rajesh Banu, Effect of extracellular polymeric substances on sludge reduction potential of *Bacillus licheniformis*, Int. J. Environ. Sci. Technol. 10 (2013) 85–92.

[7] S. Kavitha, S. Adish Kumar, K.N. Yoga lakshmi, S. Kaliappan, J. Rajesh banu, Effect of enzyme secreting bacterial pretreatment on enhancement of aerobic digestion potential of waste activated sludge interceded through EDTA, Bioresour. Technol. 150 (2013) 210–219.

[8] G. Erden, A. Filibeli, Improving anaerobic biodegradability of biological sludges by Fenton pre-treatment: Effects on single and two-stage anaerobic digestion, Desalination 251 (2009) 58–63.

[9] Y. Liu, J.H. Tay, Strategy for minimization of excess sludge production from the activated sludge process, Biotechnol. Adv. 19 (2001) 97–107.

[10] G.E.P. Box, W.G. Hunter, J.S. Hunter, Statistics for Experimenters: An Introduction to Design, Data Analysis, and Model Building, John Wiley & Sons, New York, NY, 1978.

[11] C.M. Douglas, Design and Analysis of Experiments, fifth ed., John Wiley & Sons, Singapore, 2004, pp. 150–164.

[12] APHA, Standard Methods for the Examination of Water and Wastewater, twenty-first ed., American Public Health Association, Washington, DC, 2005.

[13] S. Sayadi, N. Allouche, M. Jaoua, F. Aloui, Detrimental effects of high molecular mass polyphenols on olive mill wastewater biotreatment, Process Biochem. 35 (2000) 725–735.

[14] M.D. Labas, C.S. Zalazar, R.J. Brandi, A.E. Cassano, Reaction kinetics of bacteria disinfection employing hydrogen peroxide, Biochem. Eng. J. 38 (2008) 78–87.

[15] R. Munter, Advanced oxidation processes—Current status and prospects, Proc. Estonian Acad. Sci. Chem. 50 (2001) 59–80.

[16] S. Sahinkaya, E. Kalpici, S. Aras, Disintegration of waste activated sludge by different applications of Fenton process, Process Saf. Environ. Prot. 93 (2015) 274–281.
[17] J. Feng, X. Hu, P.L. Yue, Novel bentonite clay-based Fe-nanocomposite as a heterogeneous catalyst for photo-Fenton discoloration and mineralization of Orange II, Environ. Sci. Technol. 38 (2004) 269–275.
[18] B.R. Diego, R.C. Tatiana, C. Eduardo, J. Pires, Advanced oxidation process H2O2/UV combined with anaerobic digestion to remove chlorinated organics from bleached kraft pulp mill wastewater, Rev. Fac. Ing. Univ. Antioquia. 63 (2012) 43–54.
[19] K.Y. Park, J.W. Lee, K.H. Ahn, S.K. Maeng, J.H. Hwang, K.G. Song, Ozone disintegration of excess biomass and application to nitrogen removal, Water Environ. Res. 76 (2004) 162–167.
[20] E. Egemen, J. Corpening, N. Nirmalakhandan, Evaluation of an ozonation system for reduced waste sludge generation, Water Sci. Technol. 44 (2001) 445–452.
[21] A.G. Vlyssides, Thermal-alkaline solubilization of waste activated sludge as a pre treatment stage for anaerobic digestion, Bioresour. Technol. 91 (2004) 201–206.
[22] S. Déléris, E. Paul, J.M. Audic, M. Roustan, H. Debellefontaine, Effect of ozonation on activated sludge solubilization and mineralization, Ozone Sci. Eng. 22 (2000) 473–486.
[23] J. Fernández, J. Kiwi, C. Lizama, J. Freer, Factorial experimental design of Orange II photocatalytic discolouration, J. Photochem. Photobiol. A 151 (2002) 213–219.
[24] G. Sagawe, R.J. Brandi, D. Bahnemann, A.E. Cassano, Photocatalytic reactor for treating water pollution with solar illumination I: A simplified analysis of batch reactors, Chem. Eng. Sci. 58 (2003) 2587–2599.
[25] R.D. Bipro, N. George, B.R. Madhumita, Techno-economic evaluation of ultrasound and thermal pretreatments for enhanced anaerobic digestion of municipal waste activated sludge, Waste Manage. 32 (2012) 542–549.
[26] A.V. Ebenezer, S. Kaliappan, S. Adish Kumar, I.T. Yeom, J. Rajesh Banu, Influence of deflocculation on microwave disintegration and anaerobic biodegradability of waste activated sludge, Bioresour. Technol. 185 (2015) 194–201.
[27] T. Gayathri, S. Kavitha, S.A. Kumar, S. Kaliappan, I.T. Yeom, J. Rajesh Banu, Effect of citric acid induced deflocculation on the ultrasonic pretreatment efficiency of dairy waste activated sludge, Ultrason. Sonochem. 22 (2015) 333–340.
[28] S. Kavitha, C. Jayashree, S. Adish Kumar, S. Kaliappan, J. Rajesh Banu, Enhancing the functional and economical efficiency of a novel combined thermo chemical disperser disintegration of waste activated sludge for biogas production, Bioresour. Technol. 173 (2014) 32–41.